

Discovery of a possible X-ray counterpart to HESS J1804–216

Aya BAMBA¹, Katsuji KOYAMA², Junko S. HIRAGA¹, John P. HUGHES³, Takayoshi KOHMURA⁴,
Motohide KOKUBUN⁵, Yoshitomo MAEDA⁶, Hironori MATSUMOTO², Atsushi SENDA¹,
Tadayuki TAKAHASHI⁶, Yohko TSUBOI⁷, Shigeo YAMAUCHI⁸, Takayuki YUASA⁵

¹*RIKEN, cosmic radiation group, 2-1, Hirosawa, Wako-shi, Saitama, Japan*
bamba@crab.riken.jp

²*Department of Physics, Graduate School of Science,*
Kyoto University, Sakyo-ku, Kyoto 606-8502, Japan

³*Department of Physics and Astronomy, Rutgers University,*
136 Frelinghuysen Road, Piscataway, NJ 08854-8019, USA

⁴*kougakuin University, 2665-1, Nakano-cho, Hachioji, Tokyo 192-0015, Japan*

⁵*Department of Physics, Graduate School of Science, University of Tokyo,*
Hongo 7-3-1, Bunkyo-ku, Tokyo 113-0033, Japan

⁶*Department of High Energy Astrophysics, Institute of Space and Astronautical Science (ISAS),*
Japan Aerospace Exploration Agency (JAXA),
3-1-1 Yoshinodai, Sagami-hara, Kanagawa 229-8510, Japan

⁷*Department of Physics, Faculty of Science and Engineering, Chuo University,*
1-13-27 Kasuga, Bunkyo-ku, Tokyo 112-8551, Japan

⁸*Faculty of Humanities and Social Sciences, Iwate University,*
3-18-34 Ueda, Morioka, Iwate 020-8550, Japan

(Received 2006 July 15; accepted 2006 August 14)

Abstract

Suzaku deep observations have discovered two highly significant nonthermal X-ray sources, Suzaku J1804–2142 (Src 1) and Suzaku J1804–2140 (Src 2), positionally coincident with the unidentified TeV γ -ray source, HESS J1804–216. The X-ray sources are not time variable and show no counterpart in other wavebands, except for the TeV source. Src 1 is unresolved at Suzaku spatial resolution, whereas Src 2 is extended or composed of multiple sources. The X-ray spectra are highly absorbed, hard, and featureless, and are well fitted by absorbed power-law models with best-fit photon indices and absorption columns of $-0.3_{-0.5}^{+0.5}$ and $0.2_{-0.2}^{+2.0} \times 10^{22} \text{ cm}^{-2}$ for Src 1, and $1.7_{-1.0}^{+1.4}$ and $1.1_{-0.6}^{+1.0} \times 10^{23} \text{ cm}^{-2}$ for Src 2. The measured X-ray absorption to the latter source is significantly larger than the total Galactic neutral hydrogen column in that direction. The unabsorbed 2–10 keV band luminosities are $7.5 \times$

$10^{32}(d/5 \text{ kpc})^2 \text{ ergs s}^{-1}$ (Src 1) and $1.3 \times 10^{33}(d/5 \text{ kpc})^2 \text{ ergs s}^{-1}$ (Src 2), where d is the source distance. Among the handful of TeV sources with known X-ray counterparts, HESS J1804–216 has the largest ratio of TeV γ -ray to hard X-ray fluxes. We discuss the nature of the emission and propose the Suzaku sources as plausible counterparts to the TeV source, although further observations are necessary to confirm this.

Key words: acceleration of particles — ISM: individual (HESS J1804–216) — X-rays: ISM — X-rays: individual (Suzaku J1804–2142, Suzaku J1804–2140)

1. Introduction

The origin and acceleration mechanism of cosmic rays has remained a long-standing problem since their discovery nearly 100 years ago. The most widely accepted acceleration mechanism, at least for cosmic rays up to $10^{15.5}$ eV (the knee energy), is diffusive shock acceleration at the rims of young supernova remnants (SNRs) (e.g., Bell 1978; Blandford & Ostriker 1978). This hypothesis was greatly strengthened by the discovery of localized regions of synchrotron X-ray emission from the rims of SNR SN 1006 (Koyama et al. 1995), which indicated that SNRs were able to accelerate electrons up to \sim TeV energies. Since then, several other SNRs have been identified as electron accelerators (e.g., Koyama et al. 1997; Slane et al. 2001; Bamba et al. 2000; Bamba et al. 2001) and numerous studies have indicated that the acceleration process is very efficient (e.g., Vink & Laming 2003; Bamba et al. 2003; Bamba et al. 2005; Völk et al. 2005). Many papers regard RX J1713–3946 as a proto-type of cosmic-ray accelerating SNRs, since it is bright in both X-ray and TeV bands (Uchiyama et al. 2003). To date the best evidence for the acceleration of hadronic cosmic rays comes from observations of the Tycho SNR (Warren et al. 2005).

Recently, a TeV γ -ray telescope, High Energy Stereoscopic System (HESS), has discovered some new sources in the Galactic plane (Aharonian et al. 2005a; Aharonian et al. 2006). Some of these sources are extended on scales of ~ 0.1 , suggesting Galactic counterparts like pulsar wind nebulae (PWNe), SNRs, star-forming regions, and so on. However, their nature is still unclear: mainly because many of the new sources have no counterparts in other wavebands. They have been sometimes referred to as “dark particle accelerators”. Deep follow-up observations are crucial to elucidate their nature and hard X-ray observations are a valuable tool for this, since above a few keV we do not have to contend with absorption by the Galactic plane. The X-ray satellite Suzaku has large effective area and low background (Mitsuda et al. 2006), making it an excellent choice for such follow-up studies.

HESS J1804–216 is one of the brightest of the unidentified (unID) TeV sources (Aharonian et al. 2005a). Its size (0.2) and photon index (2.72 ± 0.06) makes it one of the largest and softest sources. Aharonian et al. (2006) proposed two possible counterparts: the ra-

dio SNR G8.7–0.1 (W30) and a young Vela-like pulsar PSR J1803–2137, although neither is a definitive identification. The HESS source overlaps only the southwestern portion of G8.7–0.1, which is about $3/4^\circ$ in diameter. The distance is estimated to be ~ 5 kpc based on associating the SNR with nearby H II regions (Kassim & Weiler 1990; Finley & Oegelman 1994). From CO observations, the surrounding region is known to be associated with molecular gas where massive star formation takes place (Ojeda-May et al. 2002). From the observed dispersion measure, PSR J1803–2137 is located at a distance of ~ 5.3 kpc (Kassim & Weiler 1990). Both candidates were detected by ROSAT (Finley & Oegelman 1994); the soft X-ray emission of G8.7–0.1 is only apparent along the northeastern radio rim. Very recently, Brogan et al. (2006) reported the discovery of a new SNR (G8.31–0.9) in this region. Swift independently discovered some X-ray sources in this region recently (Landi et al. 2006), but the statistics was quite limited due to the short observation. It is interesting to note that the AGASA and SUGAR groups have reported an excess of EeV cosmic rays from the general direction (i.e., within $\sim 20^\circ$) toward HESS J1804–216 (Hayashida et al. 1999; Bellido et al. 2001), although this result has not been confirmed by more sensitive observations by the Pierre Auger Observatory (Letessier-Selvon et al. 2005). The evidence that HESS J1804–216 is a proton accelerator therefore remains ambiguous (Fatuzzo et al. 2006).

In this paper, we report the first results of Suzaku follow-up observations of HESS 1804–216. §2 introduces the observations, our analysis is explained in §3 and we discuss our findings in §4.

2. Observations and Data Reduction

We observed a source and background region with Suzaku (Mitsuda et al. 2006), which has two sets of active instruments: four X-ray Imaging Spectrometers (XIS, Koyama et al. 2006) each at the focus of an X-Ray Telescope (XRTs, Serlemitsos et al. 2006) and a separate Hard X-ray Detector (Takahashi et al. 2006; Kokubun et al. 2006). Here, we present the analysis of XIS data only. For this study we observed both a source region (centered on the published position of HESS J1804–216 and covering the brightest part of the TeV source) and a background region some $30'$ to the southwest that avoided the TeV source (see Figure 1). Observational details are given in Table 1.

The XIS was operated in normal full-frame clocking mode in both pointings. The data reduction and analysis were made using HEADAS software version 6.0.6. We used version 0.7 processed Suzaku data, which is an internal processing applied to the Suzaku data during the science working group phase for the purpose of establishing the detector calibration as quickly as possible (for the detail, see e.g., Fujimoto et al. 2006). The XIS pulse height data for each X-ray event were converted to pulse invariant channels using the `xispi` software version 2005-12-26 and charge transfer inefficiency parameters from 2006-05-24. We filtered out data obtained during passages through the South Atlantic Anomaly or with elevation angle to the

Earth’s limb below 5° . Events with ASCA grades of 0, 2, 3, 4, and 6 were retained. The total available exposures are ~ 40 ks and ~ 43 ks for source and background, respectively.

3. Results

3.1. Images

Figure 2 shows the XIS images in the 0.5–2.0 keV (left) and 2.0–7.0 keV (right) bands. All four XIS images were combined, corrected for vignetting, and smoothed with a $\sim 20''$ (sigma) Gaussian. In the soft X-ray band, we see no significant source at the best-fit position of HESS J1804–216 (large cross). On the other hand, there are two discrete sources in the hard band image (the right panel): at positions (epoch J2000) of ($18^{\text{h}}04^{\text{m}}44^{\text{s}}, -21^{\text{d}}42^{\text{m}}42^{\text{s}}$) and ($18^{\text{h}}04^{\text{m}}34^{\text{s}}, -21^{\text{d}}40^{\text{m}}20^{\text{s}}$). We designate them as Suzaku J1804–2142 and Suzaku J1804–2140. Note that the systematic position uncertainty is about 1 arcmin. Hereafter, we will refer to these as Src 1 and Src 2, respectively. In order to examine their significance, we extracted source photons from a circle of 1.5 arcmin radius for Src 1 and 1.8 arcmin radius for Src 2 (see circles in right panel of Figure 2). The total 2.0–7.0 keV count rate was 3.7×10^{-2} cnt s $^{-1}$ and 5.3×10^{-2} cnt s $^{-1}$, respectively. The background counts in the same energy range was estimated from the background observation as 2.8×10^{-3} cnts s $^{-1}$ arcmin $^{-2}$. The significance of Src 1 and Src 2 are, then, 12.4σ and 14.9σ , respectively. The Galactic ridge emission is known to have spatial fluctuations of about 30% in intensity (Yamauchi et al. 1996; Kaneda et al. 1997). Assuming a background rate that is 30% higher than our nominal one, does not change the source detection significances critically. Data obtained at low geomagnetic cut-off rigidity (COR) values tends to have higher background, so different ranges of COR values in the source and background pointings could introduce a difference in background level. We checked the importance of this by heavily filtering on COR (allowing only values greater than 10 GV) and found that we could still detect the sources significantly even after such a drastic reduction of the data.

The spatial extent of the sources were also examined. The half power diameter of the XRT is about 2 arcmin and is almost independent of X-ray energy (Serlemitsos et al. 2006). We compared the counts within the circle of 1 arcmin radius with the counts from within a radius of 1.5 arcmin (Src 1) and 1.8 arcmin (Src 2). According to XRT calibration data the ratio of counts from a point source for these radii should be 71% and 63%. The background estimation was done in the same way as discussed above. We found that about 75% (Src 1) and 42% (Src 2) of the counts are concentrated within the 1 arcmin-radius circle. Therefore, we conclude that Src 1 is point-like or compact compared to the spatial resolution of Suzaku, whereas Src 2 is significantly extended or multiple.

Src 2 is spatially closest to the published position of HESS J1804–216 (see Figure 2), while both Src 1 and Src 2 are within the brightest parts of the TeV source. No counterparts

were found in the SIMBAD database, catalogs of H II regions (Ojeda-May et al. 2002; Kassim & Weiler 1990) and ultra-compact H II regions (Bronfman et al. 1996). Figure 1 shows the TeV γ -ray image of HESS J1804–216 (grayscale) overlaid with contours of the XIS 2.0–7.0 keV (white) and soft X-ray (ROSAT) emission (black). Both ROSAT and ASCA imaged the Suzaku XIS field of view, but failed to detect emission from either Src 1 or 2, due to low detection efficiency (ROSAT) in the hard X-ray band and strong stray light from a nearby bright source (ASCA). The Suzaku sources are quite compact compared to the HESS source. Note that PSR 1803–2137 and the previously detected soft X-ray emission from the northeastern shell of G8.7–0.1 fell outside the XIS field of view (Figure 1).

We extracted light curves for the new X-ray sources, rejecting data obtained in low COR regions (<10 GV), and applied a Kolmogorov-Smirnov test for time variability. No significant variability was detected for both sources during the observation, with the probability of constancy of 0.38 (Src 1) and 0.49 (Src 2).

3.2. Spectra

Source spectra were extracted from within circular regions of radius of 1.5 arcmin (Src 1) and 1.8 arcmin (Src 2). Background spectra were obtained from the background observation in order to account for the local Galactic ridge emission. The background spectrum was accumulated from within a 3 arcmin radius circle centered on the aim-point of this second pointing. The background rate in different observations can differ due to differences in the average COR. However our observations were done within one day of each other and the attitude of the satellite was very nearly the same. The average COR differs by only a few percent between the source and background observations, so we have ignored any effect of the COR range on the background.

As shown in Figure 3, the background-subtracted spectra are highly absorbed and featureless, so we fitted them with absorbed power-law spectral models. The absorption model used the cross sections of Morrison & McCammon (1983) with solar abundance (Anders & Grevesse 1989). We made auxiliary files for the effective area using `xissimarfgn` (Ishisaki et al. 2006), which includes the effect of contamination (Koyama et al. 2006). Figure 3 and Table 2 shows our best-fit models and parameters within 90% errors. In each case the best-fit result was acceptable statistically with reduced χ^2 values of 47.1/46 for Src 1 and 34.6/38 for Src 2. It was also possible to obtain acceptable fits using a non-equilibrium ionization thermal plasma model (Borkowski et al. 2001); however the derived temperatures, 80 (>21) keV for Src 1 and 14 (>2) keV for Src 2, were unrealistically high. We conclude that a thermal interpretation for these spectra is unlikely and favor a nonthermal interpretation instead.

Given the large mis-match in sizes between the new X-ray sources and HESS J1804–216 we also investigated how much diffuse hard X-ray emission there could be extending over the entire XIS field of view. We extracted photons from the entire field of the source pointing,

excluding Src 1 and Src 2. A background spectrum was made using all the photons in the background pointing. There was no significant excess in the source pointing compared to the background over the 2.0–10.0 keV band. Assuming a power-law model with fixed photon index ($\Gamma = 2$) and high absorption ($N_H = 10^{23} \text{ cm}^{-2}$), we obtain an absorbed flux upper limit (within a 90% error) of $5 \times 10^{-13} \text{ ergs s}^{-1} \text{ cm}^{-2}$.

4. Discussion

The new hard X-ray sources we have successfully detected with Suzaku are now the nearest potential counterparts to HESS J1804–216. Although the morphology of TeV γ -ray emission and hard X-rays are quite different, this is also the situation for the radio SNR G8.7–0.1 and the soft X-ray emission. None of the possible counterparts is a morphological match to the HESS source. Nevertheless the new X-ray sources provide interesting new information on the nature of HESS J1804–216 and the environment. An independent report (Landi et al. 2006) notices new X-ray sources in this region using Swift. The position and the flux of the source nearest to HESS J1804–216 is consistent with those of Src 2, indicating that we successfully confirmed their detection. We estimated the chance coincidence probability of unrelated X-ray sources for HESS J1804–216. With the $\log N$ - $\log S$ relation of X-ray sources in the 2.0–10.0 keV band (Sugizaki et al. 2001; Yamauchi et al. 2002; Ebisawa et al. 2005), we found that the expected number of X-ray sources is only $4\text{--}9 \times 10^{-3}$ in the elliptical region with radii of 0.016 and 0.018 degrees (the position uncertainty of the HESS source; Aharonian et al. 2006). Therefore, we concluded that they are physically associated with HESS J1804–216. In the following we discuss Src 1 and Src 2 separately.

The best-fit absorbing column for Src 1, $0.2_{-0.2}^{+2.0} \times 10^{22} \text{ cm}^{-2}$, is consistent with the Galactic neutral hydrogen column in this direction of $1.5 \times 10^{22} \text{ cm}^{-2}$ (Dickey & Lockman 1990). The unabsorbed luminosity is $7.5 \times 10^{32} (d/5 \text{ kpc})^2 \text{ ergs s}^{-1}$ in the 2.0–10.0 keV band, where d is the source distance. We quote results for a nominal value of 5 kpc although in fact we have no independent constraints on the distances to the new X-ray sources. Src 1 has a very flat spectrum, flatter than typical for young pulsars and their associated wind nebulae (PWN) (typical Γ values of 1.5 to 2.5; Possenti et al. 2002) or shell-like SNRs emitting synchrotron X-rays (typical Γ values of 2.3 to 3). Uchiyama et al. (2002) have reported a region near SNR G78.2+2.1 (Gamma-Cygni) with a photon index of 0.8–1.5, that might be comparable to Src 1. High mass X-ray binaries also have hard photon indices (Γ of 0.5–2.5; e.g. Munro et al. 2003). So Src 1 might be this type of source.

In contrast Src 2 has a best-fit absorbing column that is about an order-of-magnitude higher than the expected Galactic column. This is consistent with Src 2 being embedded in dense gas, although there are no cataloged molecular clouds in this direction. The X-ray and radio counterpart to HESS J1813–178 (Brogan et al. 2005) also appears to show evidence for excess absorption. The unabsorbed 2–10 keV band luminosity of Src 2,

$1.3 \times 10^{33}(d/5 \text{ kpc})^2 \text{ ergs s}^{-1}$, best fit photon index (see Table 2), and extended nature are all consistent with either SNR origin: a PWN or shell-like synchrotron emission.

Their origin is still unknown, but there is some interesting scenario for their nature; old SNRs colliding with molecular clouds. Yamazaki et al. (2006) argue that an old SNR shock (age of 10^5 yr) interacting with a giant molecular cloud can emit hard nonthermal X-rays and strong TeV γ -rays from shock accelerated protons through π^0 decay (see also Fatuzzo et al. 2006). They can explain large TeV γ -ray to X-ray flux ratios (factors of ~ 100). Src 2 might represent the X-ray component to the HESS source under this scenario, with the large excess absorption as a key piece of evidence.

Comparing images in other wavelengths also suggests the SNR origin. Soft X-ray emission and HESS source are both encompassed by the radio contours of G8.7–0.1, suggesting a common origin, although they do not overlap. On the other hand, the heavily absorbed Suzaku-discovered hard X-ray sources are located right at the position of peak HESS emission. The anti-correlation of HESS and ROSAT emission is likely a result of a dense region near the SNR which absorbs the soft X-rays, while at the same time enhancing the production of TeV emission from π^0 decay. The larger size of the TeV source compared to the hard X-ray source might be due to the much larger diffusion length of protons (which provide the TeV γ -rays) compared to primary electrons (which emit the hard X-rays).

HESS J1804–216 has the large ratio of TeV γ -ray to hard X-ray fluxes, which should be an important key to solve its nature. Table 3 summarizes X-ray and TeV γ -rays fluxes for a sample of TeV γ -ray emitters. Generally speaking, PWNe have rather small values of F_{TeV}/F_X , whereas SNRs tend to be brighter in TeV γ -rays. For HESS J1804–216, we assumed three counterparts; Src 1, 2, and the upper limit of the diffuse emission. We extracted the diffuse emission from the entire region of XIS FOV, whereas the TeV emission comes from wider region ($\sigma = 0.2 \text{ degree}$; Aharonian et al. 2006). Therefore, we re-normalized the flux by assuming that X-ray comes uniformly from the same region of TeV γ -rays. The flux in the TeV band is the integrated one from the entire region of the HESS source. The ratio of HESS J1804–216 is significantly larger than that of PWNe (Willingale et al. 2001; Aharonian et al. 2004a), and known shell-like SNRs emitting synchrotron X-rays (Ozaki & Koyama 1998; Aharonian et al. 2005d, for example). In fact, the F_{TeV}/F_X value is the largest among the identified objects, even if we include the upper-limit to the total hard X-ray diffuse emission from the entire XIS field of view. The value is consistent with that of HESS J1303–631, one of the new class of “dark particle accelerators” (Mukherjee & Halpern 2005; Aharonian et al. 2005f, see Table 3).

Under the assumption that the TeV γ -rays are emitted via inverse Compton on relativistic electrons, higher values of F_{TeV}/F_X suggest weaker magnetic fields, all other things being equal. Therefore, the large F_{TeV}/F_X of HESS J1804–216 suggest that the magnetic field in this source is weaker than typical in traditional PWNe and SNRs, or inverse Compton origin is unlikely.

5. Summary

Thanks to the large effective area and low background of the XIS onboard Suzaku, we have discovered two discrete X-ray sources positionally coincide with a HESS unidentified source, HESS J1804–216. The new X-ray sources have no counterpart in other wavebands, except for the TeV source. Their X-ray spectra are hard and deeply absorbed. The absorption of Src 2 significantly exceeds the Galactic value implying that it is deeply embedded in dense gas, which gives strong support to the idea that the TeV γ -rays arise from π^0 decay. Additionally the F_{TeV}/F_X value is the largest among known sources. HESS J1804–216 an important object for trying to untangle the nature of a “dark particle accelerator.”

Much remains to be done to confirm the nature of these new sources, especially in the radio band, which should be able to address the SNR origin. X-ray and TeV γ -ray observations with better spatial resolution are also needed and high time resolution will help to judge whether there is a pulsar.

6. Acknowledgements

We thank W. Hoffman, S. Funk, N. White, and P. Ubertini for fruitful discussions. We also thank all members of the Suzaku team, with our particular thanks to N. Yamasaki and the Suzaku operation team who kindly scheduled these observations. This research has made use of the SIMBAD database, operated at the CDS, Strasbourg, France. This work is supported in part by the Grant-in-Aid for Young Scientists (B) of the Ministry of Education, Culture, Sports, Science and Technology (No. 17740183). JPH acknowledges support from NASA grant NNG05GP87G.

Table 1. Observation Log.

	source	background
Date (yyyy/mm/dd)	2006/04/06	2006/04/07
Aim point (RA, Dec.)	(271.1713, -21.6759)	(270.9600, -22.0244)
Exposure (ks)	40	43

References

- Aharonian, F., et al. 2004, ApJ, 614, 897
- Aharonian, F. A., et al. 2004, Nature, 432, 75
- Aharonian, F., et al. 2005a, Science, 307, 1938
- Aharonian, F., et al. 2005b, A&A, 435, L17
- Aharonian, F., et al. 2005c, A&A, 432, L25
- Aharonian, F., et al. 2005d, A&A, 437, 135

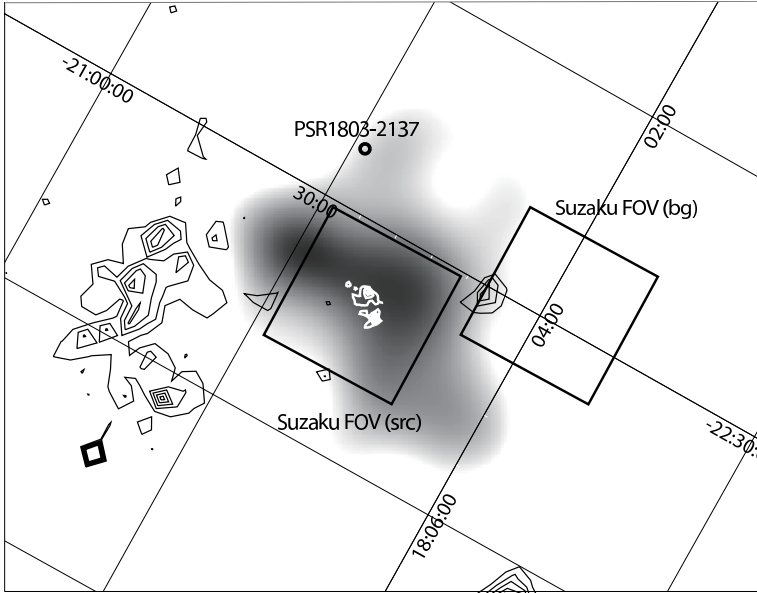


Fig. 1. HESS image (gray scale; courtesy of W. Hoffman and S. Funk) overlaid XIS 2.0–7.0 keV image (white contour), with J2000 coordinates. The black contour and circle represents ROSAT image of G8.7–0.1 (Finley & Oegelman 1994) and PSR 1803–2137. All images are in the linear scale. The black boxes show the field of views of XIS.

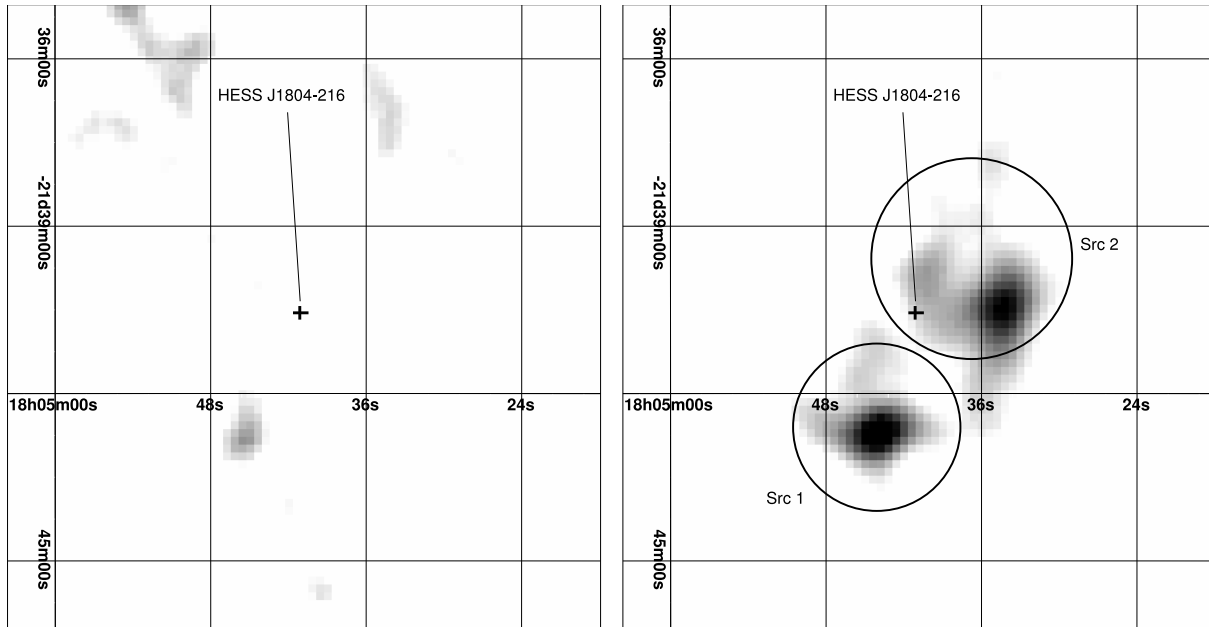


Fig. 2. XIS images of HESS J1804–216 region in the 0.5–2.0 keV band (left) and 2.0–7.0 keV band (right), with J2000 coordinates. The scales are linear. Each picture is smoothed with ~ 20 arcsec scale. The thick crosses in both panels represents the best-fit position of HESS J1804–216. The source regions used for the timing and spectral analysis are shown by thin solid lines in the right panel.

Table 2. Best-fit parameters of spectral fittings.[†]

	Src 1	Src 2
Γ	-0.3 (-0.8-0.2)	1.7 (0.7-3.1)
N_{H} [10^{22} cm ⁻²].....	0.2 (<2.2)	11 (5.3-21)
intrinsic F_{2-10} keV [‡]	2.5 (2.1-2.9)	4.3 (3.2-8.3)
observed F_{2-10} keV [‡]	2.5	2.4

[†]: Parentheses indicate single parameter 90% confidence regions.

[‡]: In the unit of 10^{-13} ergs s⁻¹ cm⁻².

Table 3. Flux ratio between X-ray and TeV γ -ray bands.

	F_X^a	F_{TeV}^b	F_{TeV}/F_X	Type ^c	Ref. ^d
Crab nebula.....	2.1×10^4	56	2.7×10^{-3}	PWN	(1) (2)
Nebula of PSR 1509.	32	16	0.5	PWN	(3) (4)
G0.9+0.1.....	5.8	2.0	0.3	PWN	(5)
SN 1006 NE	19	<2.6	<0.1	SNR	(6) (7)
RX J1713-3946.....	540	35	0.06	SNR	(8) (9)
HESS J1813-178....	7	9	1.3	SNR	(10) (11)
HESS J1303-631....	<6.4	10	>1.6	unID	(12) (13)
HESS J1804-216....	0.2 (Src 1)	6.5	33	unID	this work, (11)
HESS J1804-216....	0.4 (Src 2)	6.5	16	unID	this work, (11)
HESS J1804-216....	<0.8 (diffuse)	6.5	>8	unID	this work, (11)

^a: Unabsorbed flux in the 2-10 keV band in the unit of 10^{-12} ergs s⁻¹ cm⁻².

^b: Unabsorbed flux in the 1-10 TeV band in the unit of 10^{-12} ergs s⁻¹ cm⁻².

^c: PWN: Pulsar wind nebulae, SNR: Supernova remnants, unID: TeV unidentified sources.

^d: (1) Willingale et al. (2001); (2) Aharonian et al. (2004a); (3) DeLaney et al. (2006); (4) Aharonian et al. (2005b); (5) Aharonian et al. (2005c); (6) Ozaki & Koyama (1998); (7) Aharonian et al. (2005d); (8) Aharonian et al. (2004b); (9) Slane et al. (2001); (10) Brogan et al. (2005); (11) Aharonian et al. (2006); (12) Aharonian et al. (2005f); (13) Mukherjee & Halpern (2005);

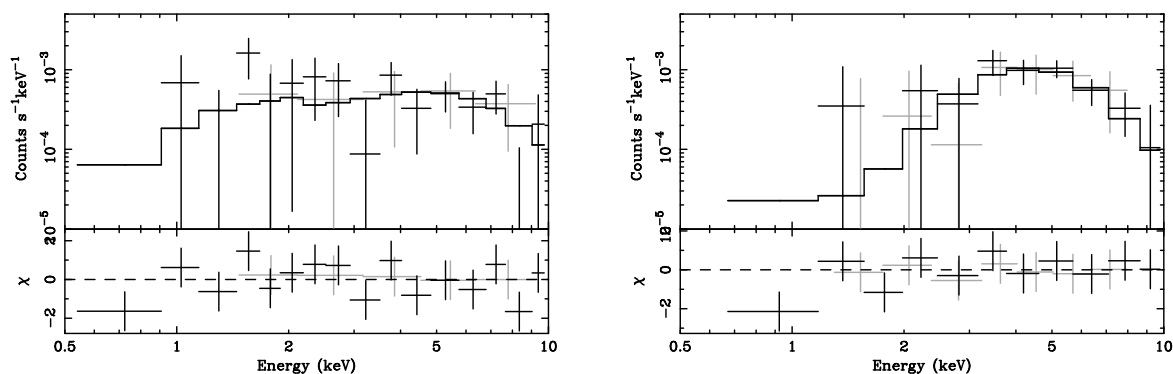


Fig. 3. Spectra of the Src 1 (left) and Src 2 (right). Gray and Black crosses represent XIS0+2+3 (added just for the clear viewing) and XIS1 data, respectively. The best-fit power-law models are shown with solid lines. Lower panels in the figures are data residuals from the best-fit models.

Aharonian, F., et al. 2005e, *A&A*, 437, L7

Aharonian, F., et al. 2005f, *A&A*, 439, 1013

Aharonian, F., et al. 2006, *ApJ*, 636, 777

Anders, E., & Grevesse, N. 1989, *Geochim. Cosmochim. Acta*, 53, 197

Bamba, A., Tomida, H., & Koyama, K. 2000, *PASJ*, 52, 1157

Bamba, A., Ueno, M., Koyama, K., & Yamauchi, S. 2001, *PASJ*, 53, L21

Bamba, A., Yamazaki, R., Ueno, M., & Koyama, K. 2003, *ApJ*, 589, 827

Bamba, A., Yamazaki, R., Yoshida, T., Terasawa, T., & Koyama, K. 2005, *ApJ*, 621, 793

Bell, A. R. 1978, *MNRAS*, 182, 443

Bellido, J. A., Clay, R. W., Dawson, B. R., & Johnston-Hollitt, M. 2001, *Astroparticle Physics*, 15, 167

Borkowski, K. J., Lyerly, W. J., & Reynolds, S. P. 2001, *ApJ*, 548, 820

Blandford, R. D., & Ostriker, J. P. 1978, *ApJ*, 221, L29

Blitz, L., Fich, M., & Stark, A. A. 1982, *ApJS*, 49, 183

Bronfman, L., Nyman, L.-A., & May, J. 1996, *A&AS*, 115, 81

Brogan, C. L., Gelfand, J. D., Gaensler, B. M., Kassim, N. E., & Lazio, T. J. W. 2006, *ApJL*, 639, L25

Brogan, C. L., Gaensler, B. M., Gelfand, J. D., Lazendic, J. S., Lazio, T. J. W., Kassim, N. E., & McClure-Griffiths, N. M. 2005, *ApJL*, 629, L105

DeLaney, T., Gaensler, B. M., Arons, J., & Pivovaroff, M. J. 2006, *ApJ*, 640, 929

Dickey, J. M., & Lockman, F. J. 1990, *ARA&A*, 28, 215

Ebisawa, K., et al. 2005, *ApJ*, 635, 214

Fatuzzo, M., Melia, F., & Crocker, R. M. 2006, *astro-ph/0602330*

Finley, J. P., & Oegelman, H. 1994, *ApJL*, 434, L25

Fujimoto, R. et al. 2006, *PASJ*, submitted

Hayashida, N., et al. 1999, *Astroparticle Physics*, 10, 303

- Ishisaki, Y. et al. 2006, PASJ, submitted
- Kaneda, H., Makishima, K., Yamauchi, S., Koyama, K., Matsuzaki, K., & Yamasaki, N. Y. 1997, ApJ, 491, 638
- Kassim, N. E., & Weiler, K. W. 1990, ApJ, 360, 184
- Koyama, K., Petre, R., Gotthelf, E.V., Hwang, U., Matura, M., Ozaki, M., & Holt S. S. 1995, Nature, 378, 255
- Koyama, K., Kinugasa, K., Matsuzaki, K., Nishiuchi, M., Sugizaki, M., Torii, K., Yamauchi, S., & Aschenbach, B. 1997, PASJ, 49, L7
- Kokubun, M. et al. 2006, PASJ, submitted
- Koyama, K. et al. 2006, PASJ, submitted
- Landi, R., et al. 2006, ApJ, in press (astro-ph/0607354)
- Letessier-Selvon, A. & Auger Collaboration 2005, 29th International Cosmic Ray Conference, Pune, 101.
- Mitsuda, K. et al. 2006, PASJ, submitted
- Morrison, R., & McCammon, D. 1983, ApJ, 270, 119
- Mukherjee, R., & Halpern, J. P. 2005, ApJ, 629, 1017
- Muno, M. P., et al. 2003, ApJ, 589, 225
- Ojeda-May, P., Kurtz, S. E., Rodríguez, L. F., Arthur, S. J., & Velázquez, P. 2002, Revista Mexicana de Astronomia y Astrofisica, 38, 111
- Ozaki, M., & Koyama, K. 1998, IAU Symp. 188: The Hot Universe, 188, 256
- Possenti, A., Cerutti, R., Colpi, M., & Mereghetti, S. 2002, A&A, 387, 993
- Serlemitsos, P. et al. 2006, PASJ, submitted
- Slane, P., Hughes, J. P., Edgar, R. J., Plucinsky, P. P., Miyata, E., & Aschenbach, B. 2001, ApJ, 548, 814
- Sugizaki, M., Mitsuda, K., Kaneda, H., Matsuzaki, K., Yamauchi, S., & Koyama, K. 2001, ApJS, 134, 77
- Takahashi, T. et al. 2006, PASJ, submitted
- Uchiyama, Y., Takahashi, T., Aharonian, F. A., & Mattox, J. R. 2002, ApJ, 571, 866
- Uchiyama, Y., Aharonian, F. A., & Takahashi, T. 2003, A&A, 400, 567
- Vink, J., & Laming, J. M. 2003, ApJ, 584, 758
- Völk, H. J., Berezhko, E. G., & Ksenofontov, L. T. 2005, A&A, 433, 229
- Warren, J. S., Hughes, J. P., Badenes, C., Ghavamian, P., McKee, C. F., Moffett, D., Plucinsky, P. P., Rakowski, C., Reynoso, E., & Slane, P. 2005, ApJ, 634, 376
- Willingale, R., Aschenbach, B., Griffiths, R. G., Sembay, S., Warwick, R. S., Becker, W., Abbey, A. F., & Bonnet-Bidaud, J.-M. 2001, A&A, 365, L212
- Yamauchi, S., et al. 2002, 8th Asian-Pacific Regional Meeting, Volume II, 81
- Yamauchi, S., Kaneda, H., Koyama, K., Makishima, K., Matsuzaki, K., Sonobe, T., Tanaka, Y., & Yamasaki, N. 1996, PASJ, 48, L15
- Yamazaki, R., Kohri, K., Bamba, A., Yoshida, T., Tsuribe, T., & Takahara, F. 2006, ApJL in press (Astro-ph/0601704)